

Supporting Information

# **Impeding Exciton-Exciton Annihilation in Monolayer WS<sub>2</sub> by Laser Irradiation**

*Yongjun Lee,<sup>1,2</sup> Ganesh Ghimire,<sup>1,2</sup> Shrawan Roy,<sup>1,2</sup> Youngbum Kim,<sup>1,2</sup> Changwon Seo,<sup>1,2</sup>  
Ajay K. Sood,<sup>3</sup> Joon I. Jang,<sup>4</sup> and Jeongyong Kim<sup>1,2</sup>*

<sup>1</sup>Department of Energy Science, Sungkyunkwan University, Suwon 16419, Republic of Korea

<sup>2</sup>Center for Integrated Nanostructure Physics, Institute for Basic Science, Suwon 16419, Republic of Korea

<sup>3</sup>Department of Physics, Indian Institute of Science, Bangalore-560012, India

<sup>4</sup>Department of Physics, Sogang University, Seoul 04107, Republic of Korea

**Corresponding Author**

\*J. Kim ([j.kim@skku.edu](mailto:j.kim@skku.edu))

**Spectral fitting of the PL from 1L-WS<sub>2</sub> monitored during laser irradiation.**

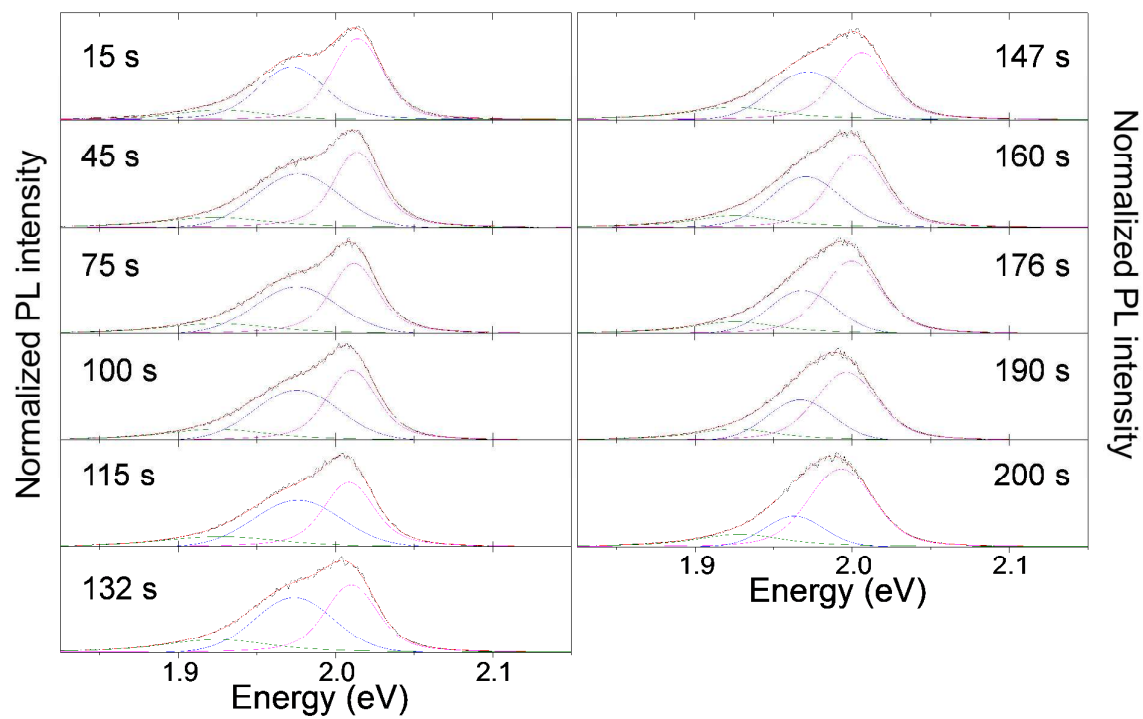


**Figure S1.** Fitting results of the PL spectra shown in Figure 1a in the main text.

Another observation of the PL enhancement by laser irradiation.

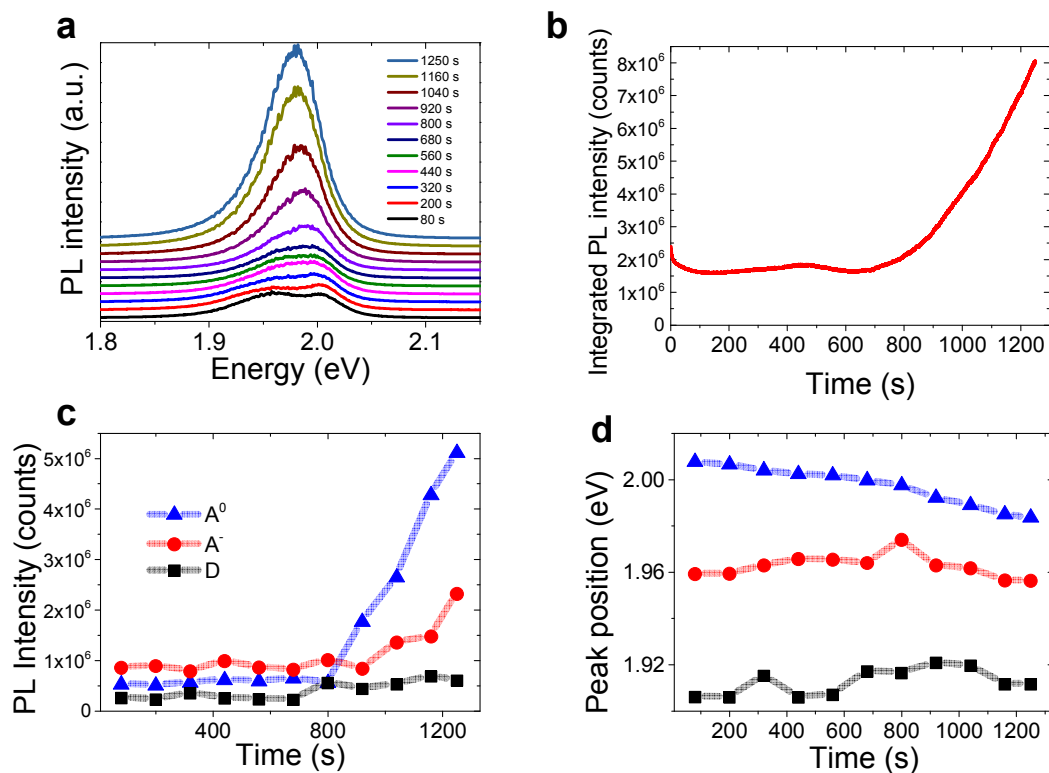


**Figure S2.** (a) PL spectra obtained under various laser irradiation times, showing the change of the PL shape. (b) Plot of the PL intensity as a function of laser irradiation time. (c) PL intensities and (d) peak positions of each excitonic matter as a function of irradiation time.

### PL peak shift in ME 1L-WS<sub>2</sub> in air and vacuum environments

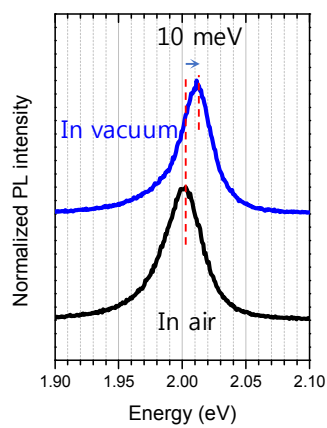


**Figure S3.** PL peak shift in ME 1L-WS<sub>2</sub> in air (black) and vacuum (blue). The PL spectra were obtained at the same position within a single sample.

**Variation of the PL characteristics under laser irradiation in Ar environment.**

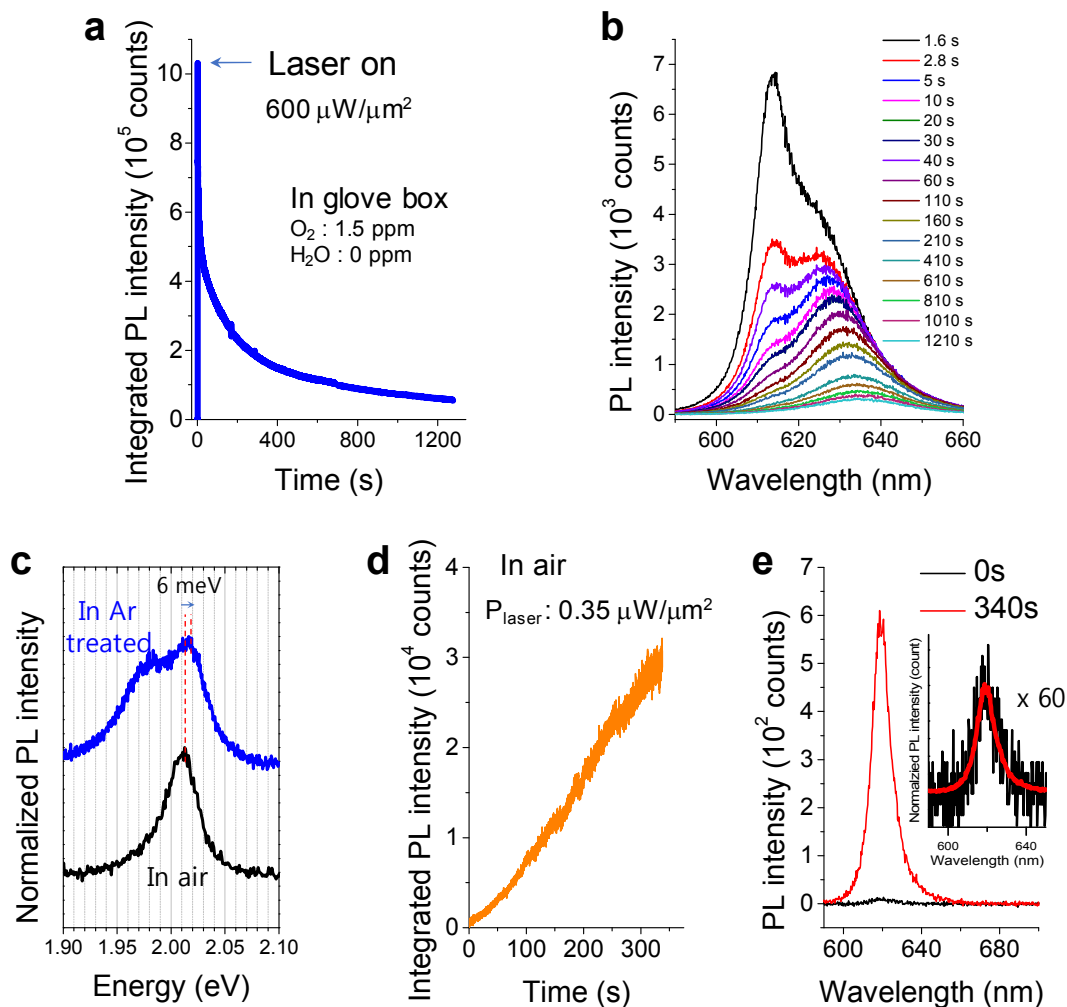


**Figure S4.** (a) Integrated PL intensity and (b) PL spectra of 1L-WS<sub>2</sub> as a function of laser irradiation time at  $\sim 600 \mu\text{W}/\mu\text{m}^2$ . (c) PL spectrum in Ar environment (glove box) after laser irradiation (blue). The black spectrum was measured from the same sample when exposed in air (outside the glove box). (d) Integrated PL intensity as a function of laser irradiation time at  $\sim 0.35 \mu\text{W}/\mu\text{m}^2$  in air. The sample was pre-irradiated in Ar environment. Note that this power is 3 orders of magnitude lower than that used for laser irradiation in Ar environment. (e) PL spectra taken in air with laser irradiation times of 0 s (black) and 340 s (red). Inset shows the PL intensity increase by 60 times during laser irradiation.

### **Estimation of quantum yield of the sample.**

We followed the previous protocols of estimating quantum yields (QY) of 1L-TMDs using rhodamine-6G dye molecules as reference sample with 100 % QY.<sup>1,2</sup> We prepared various concentrations of rhodamine-6G molecules in methanol and then measured PL and absorbance of them and found that 3  $\mu\text{M}$  is the optimal concentration of rhodamine-6G. By comparing the PL and absorption intensities of 1L-WS<sub>2</sub> samples and the rhodamine-6G solution, we determined the QYs of our 1L-WS<sub>2</sub> samples. The measured QY of ME pristine 1L-WS<sub>2</sub> was ~8 %, which is in the range of previously reported QY values of 1L-WS<sub>2</sub>.<sup>2-3</sup>

### Calculation of the densities of photo-excited excitons.

To calculate the densities of photo-excited excitons, we employed the same calculation method used in our previous report.<sup>4</sup> By assuming that every absorbed photon creates one exciton, the exciton densities undergoing non-radiative ( $N_n$ ) and radiative ( $N_r$ ) recombination are given by

$$N_n = a(1-Q)\left(\frac{I}{E}\right)t_n \quad (1)$$

$$N_r = aQ\left(\frac{I}{E}\right)t_r \quad (2)$$

Here,  $a$  is the absorption efficiency of 1L-WS<sub>2</sub> at 532 nm, 3%,<sup>4</sup>  $Q$  is the PL quantum yield of 1L-WS<sub>2</sub>, 6%,<sup>2</sup>  $I$  is the excitation intensity,  $E$  is the energy of laser light,  $3.72 \times 10^{19}$  J,  $t_n$  and  $t_r$  are non-radiative (= 900 ps) and radiative recombination (13 ns) times, respectively.<sup>2</sup> The total density of photo-excited excitons is the sum of  $N_n$  and  $N_r$ . If we apply  $1 \mu\text{W}/\mu\text{m}^2$  of the excitation intensity, the calculated total density of photo-excited excitons is  $1.31 \times 10^{10} \text{ cm}^{-2}$ .

### Discussion for other excitonic matter.

We conducted wavelength-dependent TRPL to separately measure lifetimes of excitons, trions or defect trapped excitons. We found that there were no significant differences in lifetime at each center wavelength. However, the formation of trions or biexcitons with increasing the excitation level should be considered. The formation of biexcitons in monolayer TMDs have been reported at high excitation levels.<sup>5-6</sup> Within our experimental range, however, the shape of the PL spectra is unchanged, suggesting that the formation of other excitonic matter could be neglected.

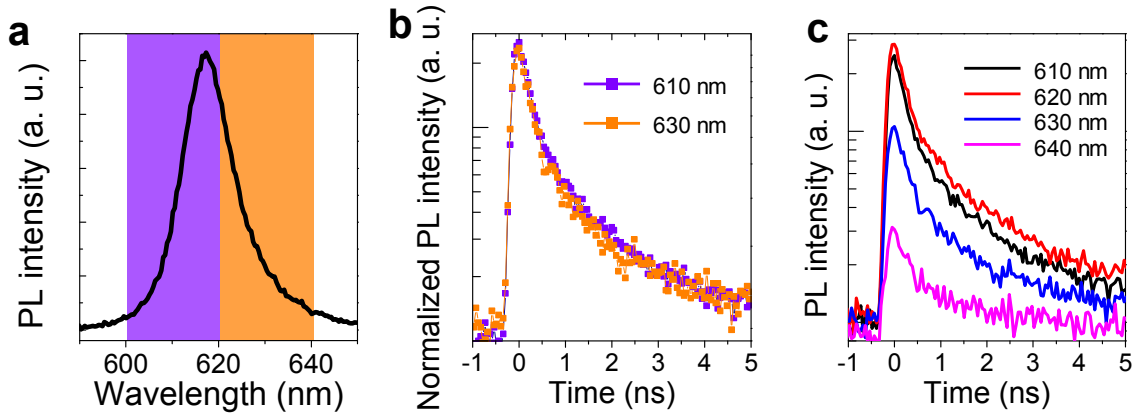


**Figure S5.** (a) PL spectrum of 1L-WS<sub>2</sub> at 1  $\mu\text{J}/\text{cm}^2$  (b) Normalized time-resolved PL (TRPL) curves at two center wavelengths, 610 nm (violet) and 630 nm (orange), where the spectral monitoring ranges are marked in (a) with the same colors. (c) TRPL curves at various center wavelengths.

A TRPL detector was connected to a monochromator and a grating in the monochromator was electrically controlled to adjust the center wavelength. The diffracted light by the grating reached to an adjustable slit placed in front of a photo-detector. The width of the detection wavelength was 20 nm adjusted by the size of the monochromator input slit.

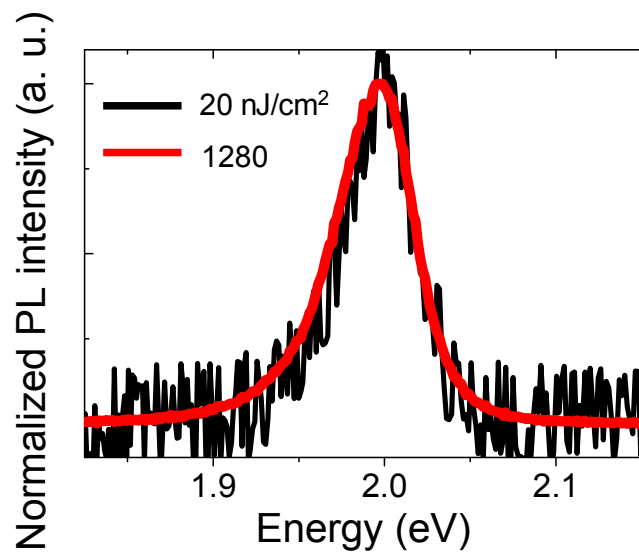


**Figure S6.** PL spectra of the sample used for the TRPL measurement in Figure 4 of the main text.

## Evolution of the PL spectra upon laser irradiation in a vacuum chamber

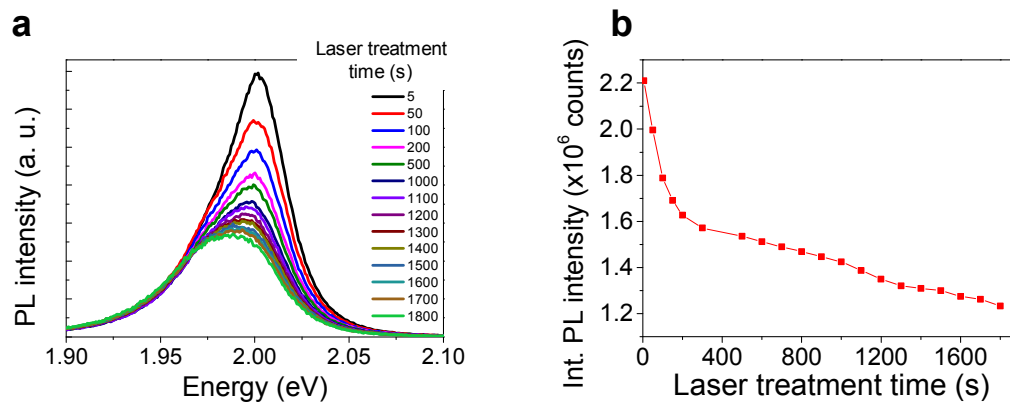


**Figure S7.** (a) PL spectra and (b) the corresponding PL intensities as a function of laser irradiation time. It is evident that the trion portion increases with the laser-exposure time.

**Variation of PL and Raman intensities by 488 nm laser irradiation.**

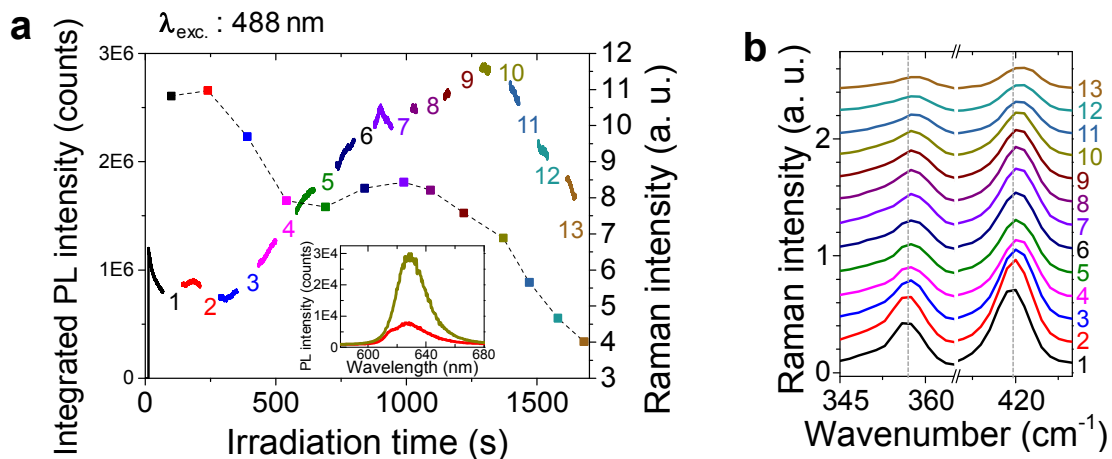


**Figure S8.** (a) Plot of the PL (line with numeric) and Raman (dots with dotted line for guide the eye) intensities as a function of laser irradiation time. Inset shows the PL spectra before (100 s, red trace) and after (1400 s, dark yellow trace) PL enhancement. (b) Time evolution of Raman spectra of 1L-WS<sub>2</sub>. The numbers in the right-side axis indicates the time when they were measured as marked in (a) with same numbering and colors. Two main peaks, E<sub>2g</sub> and A<sub>1g</sub> peaks, are shown at ~ 357 cm<sup>-1</sup> and ~ 417 cm<sup>-1</sup>, respectively.

## REFERENCES

- (1) Mak, K. F.; Lee, C.; Hone, J.; Shan, J.; Heinz, T. F., Atomically Thin MoS<sub>2</sub>: A New Direct-Gap Semiconductor. *Phys. Rev. Lett.* **2010**, 105 (13), 136805.
- (2) Yuan, L.; Huang, L., Exciton dynamics and annihilation in WS<sub>2</sub> 2D semiconductors. *Nanoscale* **2015**, 7 (16), 7402-7408.
- (3) Amani, M.; Taheri, P.; Addou, R.; Ahn, G. H.; Kiriya, D.; Lien, D.-H.; Ager, J. W.; Wallace, R. M.; Javey, A., Recombination Kinetics and Effects of Superacid Treatment in Sulfur- and Selenium-Based Transition Metal Dichalcogenides. *Nano Lett.* **2016**, 16 (4), 2786-2791.
- (4) Lee, Y.; Yun, S. J.; Kim, Y.; Kim, M. S.; Han, G. H.; Sood, A. K.; Kim, J., Near-field spectral mapping of individual exciton complexes of monolayer WS<sub>2</sub> correlated with local defects and charge population. *Nanoscale* **2017**, 9 (6), 2272-2278.
- (5) You, Y.; Zhang, X.-X.; Berkelbach, T. C.; Hybertsen, M. S.; Reichman, D. R.; Heinz, T. F., Observation of biexcitons in monolayer WSe<sub>2</sub>. *Nat. Phys.* **2015**, 11 (6), 477-481.
- (6) Kim, M. S.; Yun, S. J.; Lee, Y.; Seo, C.; Han, G. H.; Kim, K. K.; Lee, Y. H.; Kim, J., Biexciton Emission from Edges and Grain Boundaries of Triangular WS<sub>2</sub> Monolayers. *ACS Nano* **2016**, 10 (2), 2399-2405.